# CYP2J2 Overexpression Increases EETs and Protects against Angiotensin II-Induced Abdominal Aortic Aneurysm in Mice

Zhejun Cai, Gang Zhao, Jiangtao Yan, Wanjun Liu, Wenjing Feng, Ben Ma, Lei Yang, Jian-An Wang, Jian-an Wang, Ling Tu and Dao Wen Wang

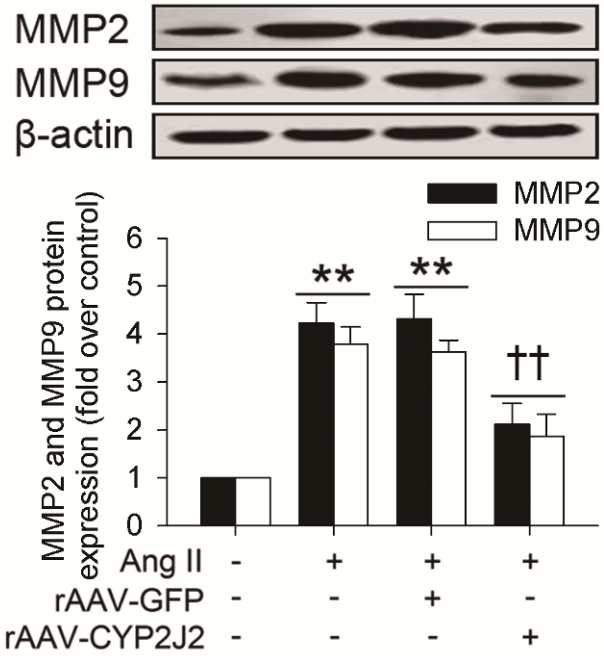


**Figure S1. rAAV-CYP2J2 delivery reduced aortic MMPs expression induced by Ang II infusion in ApoE$^{-/-}$ mice.** Western blot analysis showed that CYP2J2 overexpression reduced MMP2 and MMP9 expression in the aortic tissues of ApoE$^{-/-}$ mice 8 weeks after rAAV-CYP2J2 injection (n=8 for each group; ** *P*<0.01 *vs*. control; $^{\dagger\dagger}$ *P*<0.01 *vs*. Ang II + rAAV-GFP).

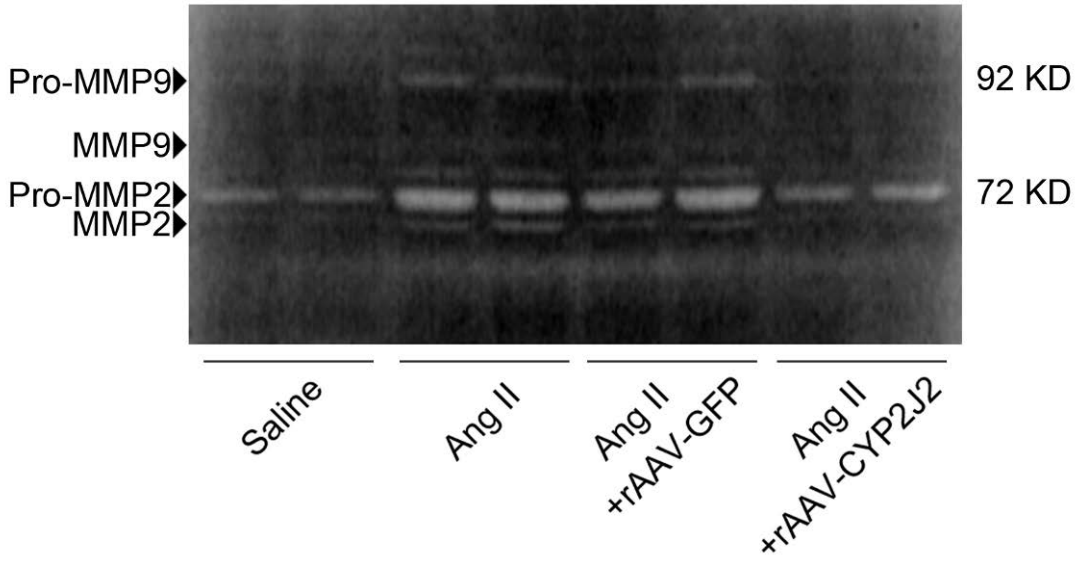


**Figure S2. CYP2J2 overexpression reduced aortic MMPs activities induced by Ang II infusion in ApoE$^{-/-}$ mice.** Gelatin zymographic analysis showed that CYP2J2 overexpression reduced MMP2 and MMP9 activities in the aortic tissues of ApoE$^{-/-}$ mice 8 weeks after rAAV-CYP2J2 injection.

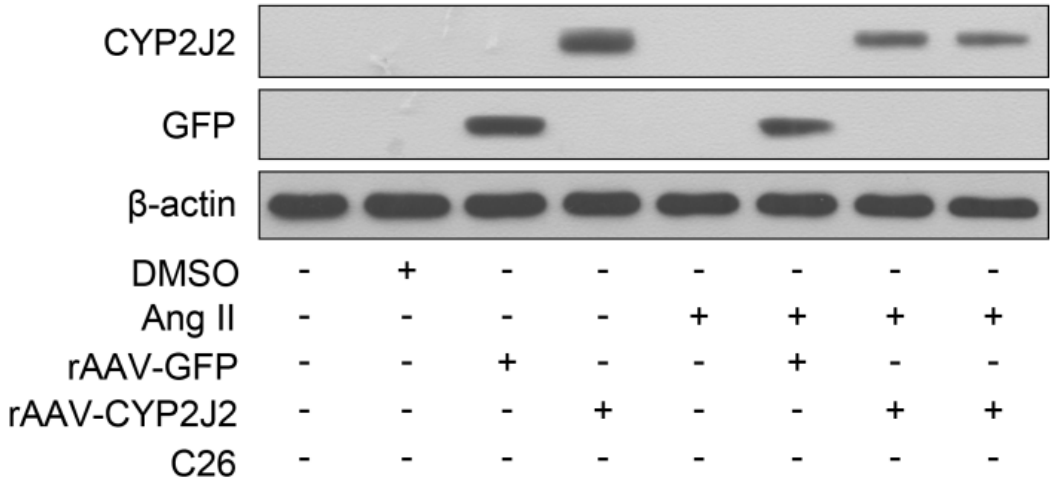


**Figure S3. rAAV-CYP2J2 transfection significantly induced CYP2J2 expression in VSMC.** Western blot analysis showed that rAAV-CYP2J2 and rAAV-GFP transfection significantly induced corresponding CYP2J2 and GFP expression in VSMC, respectively.

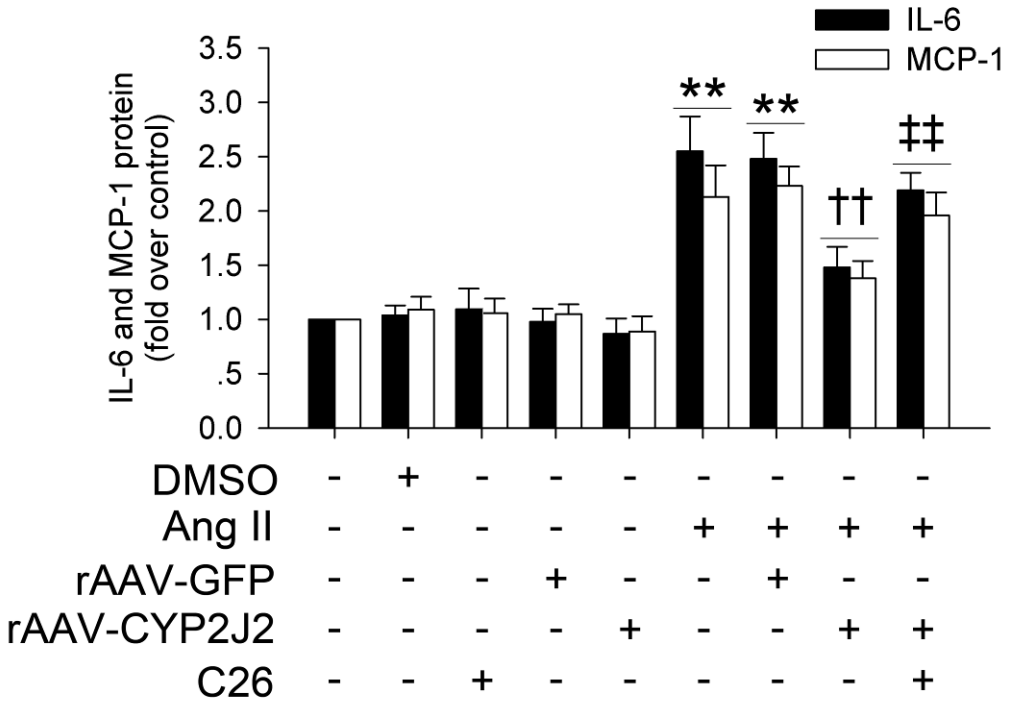


**Figure S4. rAAV-mediated CYP2J2 overexpression suppressed Ang II-induced inflammatory cytokines expression in VSMCs.** ELISA analysis showed that rAAV-CYP2J2 transfection significantly reduced inflammatory cytokines IL-6 and MCP-1 expression induced by Ang II (10 μmol/l) in VSMCs. However, the selective CYP2J2 inhibitor, C26 (10 μmol/l), markedly inhibited the effect of CYP2J2 overexpression (n=3 for each experiment; ** $P$<0.01 *vs*. control; $^{††}$ $P$<0.01 *vs*. Ang II + rAAV-GFP; $^{‡‡}$ $P$<0.01 *vs*. Ang II + rAAV-CYP2J2).

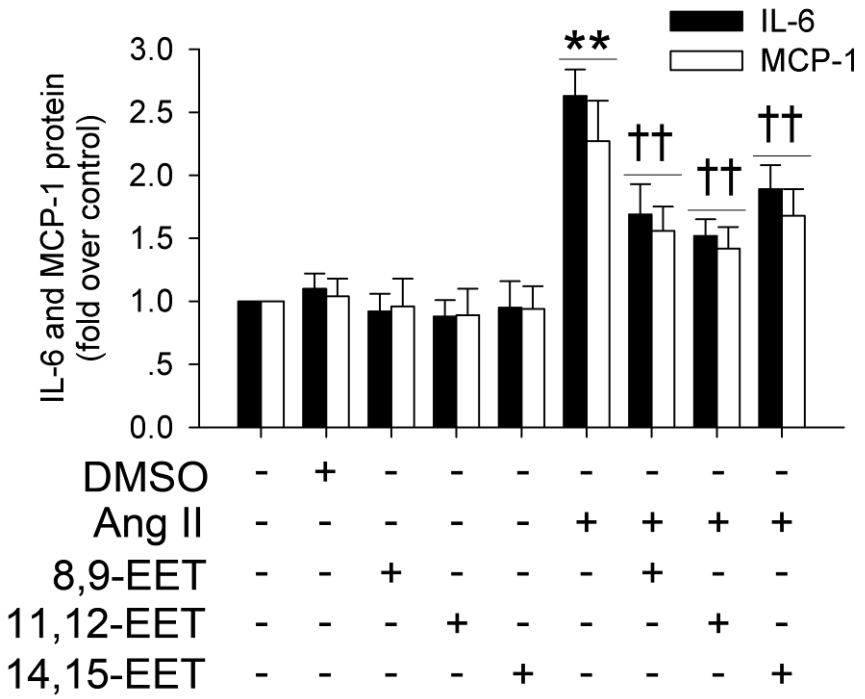


**Figure S5. EETs suppressed Ang II-induced inflammatory cytokines expression in VSMCs.** CYP2J2 metabolites, 10 μmol/l of 8,9-, 11,12-, and 14,15-EETs could all suppressed Ang II (10 μmol/l) induced increase in IL-6 and MCP-1 expression in VSMCs assessed by ELISA, and 11,12-EET exhibited the most profound effect (n=3 for each experiment; ** $P$<0.01 *vs*. control; †† $P$<0.01 *vs*. Ang II).

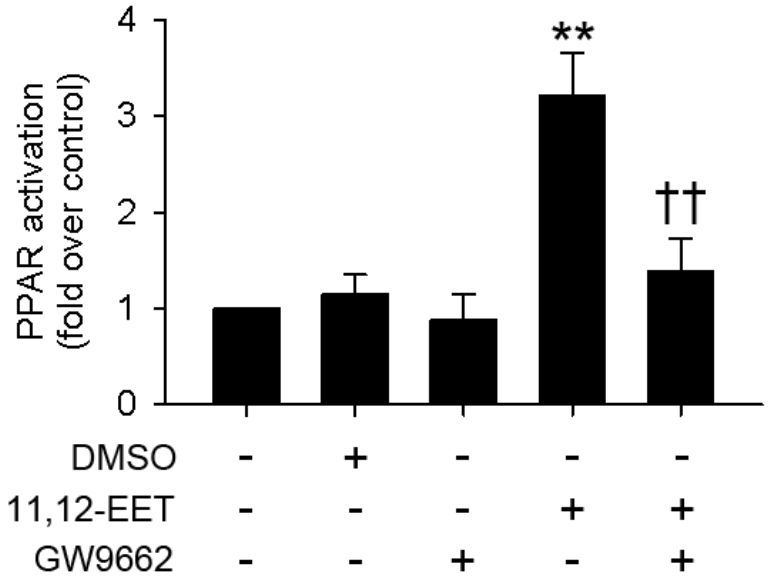


**Figure S6. 11,12-EET synergized with PPARγ transection to induce PPAR reporter gene activation in HEK293 cells.** HEK293 cells were transfected with pcDNA-PPARγ**.** 11,12-EET markedly induced PPAR reporter gene activation, while PPARγ antagonist GW9662 (1 μmol/l) significantly abolished this effect (n=3 for each experiment; ** *P*<0.01 *vs*. control; $^{\dagger\dagger}$ *P*<0.01 *vs*. 11,12-EET).

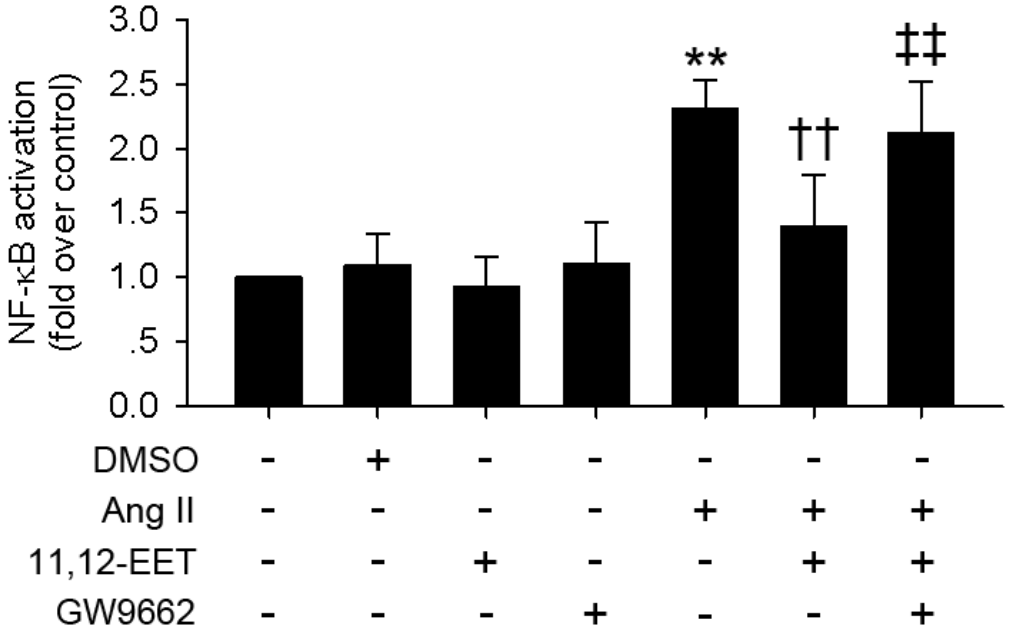


**Figure S7. The protective effect of 11,12-EET on NF-κB activation is mediated by PPARγ in HEK293 cells.** 11,12-EET (100 nmol/l) incubation markedly reduced Ang II (10 μmol/l) induced NF-κB reporter gene activation, while PPARγ antagonist GW9662 (1 μmol/l) markedly inhibited this effect (n=3 for each experiment, ** $P<0.01$ *vs*. control; $^{\dagger\dagger}$ $P<0.01$ *vs*. Ang II; $^{\ddagger\ddagger}$ $P<0.01$ *vs*. Ang II + 11,12-EET).

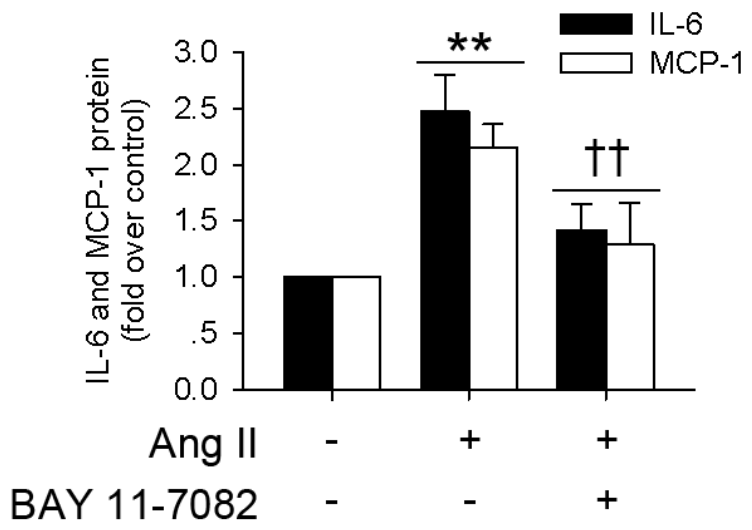


**Figure S8. NF-κB signaling mediates Ang II induced inflammatory cytokines expression in VSMCs.** ELISA analysis showed that NF-κB inhibitor BAY 11-7082 (10 μmol/l) significantly blocked the increase in IL-6 and MCP-1 expression stimulated by Ang II (10 μmol/l) incubation in VSMCs (n=3 for each experiment; ** $P<0.01$ *vs*. control; $^{\dagger\dagger}$ $P<0.01$ *vs*. Ang II).